

Nonequilibrium and current sheet formation in line-tied magnetic fields

C. S. Ng and A. Bhattacharjee

Department of Physics and Astronomy, The University of Iowa, Iowa City, Iowa 52242

(Received 12 May 1998; accepted 24 July 1998)

Parker's model of coronal heating [E. N. Parker, *Astrophys. J.* **174**, 499 (1972)] is considered within the framework of ideal reduced magnetohydrodynamics. It is shown that there can be at most one smooth magnetostatic equilibrium for a given smooth footpoint mapping between two end plates to which field lines are line-tied. If such a smooth equilibrium is deformed continuously by further footpoint motion so that it becomes unstable, there is no other smooth equilibrium for the plasma to relax to, and the system tends to a nonequilibrium state containing singular currents ("current sheets"). It is shown that this process can occur as the system relaxes asymptotically to a state of minimum energy (possibly in infinite time). Numerical simulations that begin from smooth initial conditions containing current layers are presented. As the current layers become increasingly intense due to footpoint motion and eventually cross a threshold for instability, the magnetic relaxation observed in the simulation shows a tendency to form nonequilibrium states with current sheets. A necessary geometrical criterion that determines the sites of current sheet formation in models without nulls or closed field lines is given. According to this criterion, the rate of velocity amplification, analogous to the Lyapunov exponent in nonlinear dynamics, becomes unbounded at singularities. © 1998 American Institute of Physics. [S1070-664X(98)01411-6]

"A not uncommon phenomenon in science is the rapid transition, without apparent cause, from one state in which a concept is almost universally disbelieved and rejected to another state in which it is so transparent as to require no comment and exhibit no visible history. Sometimes there may be a transitional period during which both states coexist simultaneously (and schizoidally) in the scientific community. It is my belief that the subject of this paper is either in the course of a transition or close to it (but in which state it lies preponderantly, I am not willing to guess)."

—H. Grad, in *Proceedings of the Workshop on Mathematical Aspects of Fluid and Plasma Dynamics*, Trieste, 1984 (Università Degli Studi Di Trieste, Facoltà Di Scienze, Istituto Di Meccanica), pp. 253–282.

I. INTRODUCTION

About 25 years ago, Parker proposed that a large-scale solar coronal magnetic field with a complicated topology does not possess a smooth magnetostatic equilibrium.¹ In Parker's model, the solar corona is treated as an ideal plasma column, bounded by two perfectly conducting end plates at $z=0$ and $z=L$, representing the photosphere. The footpoints of the magnetic field in the photosphere are frozen ("line-tied"). Initially, there is a uniform magnetic field along the z direction. Keeping the footpoints of the magnetic field on one of the plates ($z=0$) fixed, the footpoints on the other plate ($z=L$) are subjected to slow, random motions that deform the initially uniform magnetic field. The footpoint motions are assumed to take place on a time scale much longer than the characteristic time for Alfvén wave propagation be-

tween $z=0$ and $z=L$, so that the plasma can be assumed to be in static equilibrium nearly everywhere, if such equilibrium exists.

For a given equilibrium, a footpoint mapping can be defined by following field lines from one plate to the other. Since the plasma is assumed to obey the ideal magnetohydrodynamic (MHD) equations, the magnetic field lines are frozen in the plasma and cannot be broken during the footpoint motions. Therefore the footpoint mapping must be continuous for smooth footpoint motion. Parker claimed that if a sequence of random footpoint motions renders the mapping sufficiently complicated, there will be no smooth equilibrium for the plasma to relax to, and tangential discontinuities of the magnetic field ("current sheets") must develop.¹

Parker's claim has stimulated considerable debate that continues to this day.^{2–5} (For a review and extensive references, see Refs. 6–8.) The Parker problem is nonstandard, and in the mathematical literature there appear to be very few rigorous results that are directly applicable. Parker himself has given several physically persuasive arguments⁸ in support of his claim, but a mathematically rigorous demonstration of current sheet solutions, based on the ideal MHD equations, continues to be elusive.

The first significant objections to Parker's claim of nonequilibrium were raised by van Ballegooijen² (hereafter, VB) who argued that smooth equilibria must always exist as long as the footpoint motion is smooth (or continuous). Furthermore, based on certain assumptions regarding the geometric structure of current sheets, VB claimed that an equilibrium current sheet cannot be reconciled with a continuous footpoint mapping. (VB's argument, valid for force-free plasmas, was later extended to plasmas with finite pressure gradients by Field.⁹)

While VB's treatment of Parker's model shows that non-

symmetric smooth solutions do exist for smooth footpoint motions, it leaves unanswered the question: what will occur if a smooth equilibrium is gradually twisted so that it eventually becomes unstable? This question has been considered recently by Longcope and Strauss,⁵ and involves an important point of principle: does the unstable, line-tied corona represented in Parker's idealized model tend to a nonequilibrium state with a true current singularity or to an equilibrium with an "intense, but ultimately continuous, current layer?"⁵

Numerical simulations seem to suggest that current sheets can appear after an equilibrium becomes unstable.¹⁰⁻¹⁷ Illuminating as these simulations are, there are two reasons why it is impossible to settle the debated point of principle entirely on the basis of numerical evidence. First, even if the system tends to a true current singularity, the singularity may not be realized in finite time. (For some examples of infinite-time current singularities in systems with well-defined separatrices, see Ref. 18 and other citations therein.) Needless to say, an infinite-time singularity can never be realized by a computer code running for finite time, no matter how accurate the code may be. Second, limitations of spatial resolution make it extremely difficult, if not impossible, to distinguish between a current sheet and a very thin current layer. It may be argued that for all practical purposes this distinction is of academic interest because once the current density does become very intense, a small but finite dissipation will intervene to regularize a potential singularity and transform it to a current layer. This argument should be treated with caution, because the *tendency* of formation of a true singularity (be it finite-time or infinite-time) has fundamental and broader consequences for the reconnection and turbulent dynamics of coronal plasmas in the limit of zero dissipation. It is, therefore, worthwhile to pursue the question of principle raised by Longcope and Strauss.⁵

Building on VB's original argument, Longcope and Strauss claim that the line-tying constraint is incompatible with a genuine current sheet. They begin from a smooth initial force-free equilibrium that is unstable to a line-tied variant of the ideal coalescence instability¹⁹ and proceed to investigate the nature of the final state after the instability has run its course. They *assume* that in the presence of viscosity the system must relax to a new force-free equilibrium of minimum magnetic energy, although the existence of such a second equilibrium is not shown rigorously. Based on the reduced MHD equations (presented in Sec. II), we show in Sec. III that this situation also admits another possibility: an unstable system may relax to a nonequilibrium state with a current sheet which is also a state of minimum energy. This leads us naturally to the question: which of these two possibilities is actually realized in Parker's model?

To answer this question, we present a new theorem: *there is at most one smooth equilibrium for any given smooth footpoint mapping*. It follows from this theorem that if there exists a smooth but unstable equilibrium for a given smooth footpoint mapping, there is no other smooth equilibrium that the unstable plasma can relax to. Thus nonequilibrium with current sheets must develop, consistent with the original suggestion of Parker.¹

In Sec. IV we present some numerical simulations for the line-tied coalescence instability as well as equilibria containing thin and intense current layers which become ideally unstable when the current density in the layers exceeds a certain threshold. The numerical evidence appears to be qualitatively consistent with our claim that in the aftermath of the instability, the system tends to a nonequilibrium state with a current sheet.

Parker's model presents a difficult challenge for MHD theory because its line-tied geometry does not fit neatly into any of the well-known categories of field-line geometry where the formation of current sheets is well established. These categories include systems with closed field lines (cf. Ref. 20), two-dimensional systems with *X*-type neutral lines (cf. Ref. 18) or three-dimensional systems with magnetic nulls (cf. Refs. 21 and 22), all of which have well-defined magnetic separatrices. There are no obvious separatrices in Parker's model because the field lines have finite length and no continuous symmetry, do not close on themselves, and do not appear to develop nulls. We demonstrate in Sec. V that a necessary condition for the location of current singularities in Parker's model is where the exponent representing the rate of velocity amplification, defined by Greene,²³ tends to arbitrarily large values. Thus current singularities in three-dimensional (3D) geometry can be associated with sites of unbounded increase of the velocity amplification coefficient, analogous to the well-known Lyapunov exponent in nonlinear dynamics. We conclude in Sec. VI with a summary.

II. MODEL AND EQUATIONS

We consider Parker's model¹ of the solar corona within the framework of the reduced MHD (RMHD) equations^{2,24}

$$\frac{\partial \Omega}{\partial t} + [\phi, \Omega] = \frac{\partial J}{\partial z} + [A, J] + \nu \nabla_{\perp}^2 \Omega, \quad (1)$$

$$\frac{\partial A}{\partial t} + [\phi, A] = \frac{\partial \phi}{\partial z} + \eta \nabla_{\perp}^2 A, \quad (2)$$

where $\mathbf{B} = \hat{\mathbf{z}} + \mathbf{B}_{\perp} = \hat{\mathbf{z}} + \nabla_{\perp} A \times \hat{\mathbf{z}}$ is the magnetic field, $\mathbf{v} = \nabla_{\perp} \phi \times \hat{\mathbf{z}}$ is the fluid velocity, $\Omega = -\nabla_{\perp}^2 \phi$ is the *z*-component of the vorticity, $J = -\nabla_{\perp}^2 A$ is the *z*-component of the current density, $[\phi, A] \equiv \phi_y A_x - \phi_x A_y$, η is the resistivity, and ν is the viscosity. As discussed in Sec. I, we assume that the field lines are line-tied at $z=0$ and $z=L$.

An ideal magnetostatic equilibrium solution of Eqs. (1) and (2) is obtained by setting all explicitly time-dependent terms as well as ϕ and η to zero. We then obtain

$$\frac{\partial J}{\partial z} + [A, J] = 0. \quad (3)$$

Equation (3), which can also be written as $\mathbf{B} \cdot \nabla J = 0$, implies that the current density J must be constant along a given magnetic field line in an ideal magnetostatic equilibrium.

Equation (3) is isomorphic to the incompressible two-dimensional (2-D) Euler equation in hydrodynamics if we identify z as a time variable, A as a stream function and J as the vorticity field. This allows us to invoke a well-known existence theorem²⁵ to assert that for any smooth function

$A(x,y,0)$, a smooth and unique equilibrium solution satisfying Eq. (3) can be found in a bounded domain, assuming that the velocity on the boundary curve (in the x,y plane) is finite. Such an equilibrium solution defines a continuous mapping of the footpoint of a field line from $z=0$ onto $z=L$,

$$\mathbf{x}_\perp(z) = \mathbf{X}[\mathbf{x}_\perp(0), z], \quad \mathbf{x}_\perp(L) = \mathbf{X}[\mathbf{x}_\perp(0), L], \quad (4)$$

where $\mathbf{x}_\perp = (x,y)$, $\mathbf{X} = (X,Y)$. The mapping can be found by tracing field lines from $z=0$ to $z=L$ according to the Hamiltonian equations

$$\frac{dX}{dz} = \frac{\partial A}{\partial y}(X,Y,z), \quad \frac{dY}{dz} = -\frac{\partial A}{\partial x}(X,Y,z), \quad (5)$$

with given initial condition $\mathbf{x}_\perp(0)$.

VB claimed that for every ideal equilibrium satisfying Eq. (3) with smooth A and J , a neighboring smooth equilibrium can be found for all time by specifying smooth boundary flows $\phi(x,y,0,t)$ and $\phi(x,y,L,t)$ at the two end plates. He demonstrated this by deriving an equation (hereafter, referred to as the VB equation) for the stream function $\phi(x,y,z,t)$. The VB equation is obtained by assuming that Eq. (3) holds for all time, taking its time derivative, and then eliminating the time-derivatives using Eq. (2):

$$\begin{aligned} \frac{\partial}{\partial z} \left\{ \frac{\partial \Omega}{\partial z} + \nabla_\perp^2[\phi, A] \right\} + \left[\frac{\partial \phi}{\partial z} + [A, \phi], J \right] \\ + \left[A, \frac{\partial \Omega}{\partial z} + \nabla_\perp^2[\phi, A] \right] = 0. \end{aligned} \quad (6)$$

Here it is assumed that the plasma is ideal (that is, $\eta=0$). Since Eq. (6) is linear in ϕ and second order in $\partial/\partial z$, it is plausible that a smooth solution of $\phi(x,y,z,t)$ can be found by specifying the boundary conditions $\phi(x,y,0,t)$ and $\phi(x,y,L,t)$ for all smooth functions A and J satisfying Eq. (3). Once such a smooth solution $\phi(x,y,z,t)$ is obtained, a smooth equilibrium $A(x,y,z,t)$ can be found for all time by solving Eq. (2). VB argued that the only way in which $A(x,y,z,t)$ may lose its smoothness is if the velocity field at the boundary, specified by $\phi(x,y,0,t)$ and $\phi(x,y,L,t)$, is discontinuous.

Since the VB equation is a partial differential equation with fourth-order spatial derivatives and unknown coefficients involving $A(x,y,z,t)$, the issues of existence and uniqueness for the two-point boundary value problem are nontrivial. We discuss some of the relevant mathematical issues in Appendix A (when periodic boundary conditions in \mathbf{x}_\perp are imposed). Let us assume that the conditions for the existence of a smooth equilibrium solution of the VB equation are fulfilled for a given footpoint mapping. Even if that is so, such an equilibrium can be gradually deformed by further footpoint motions and eventually driven unstable if the imposed twist (and/or shear) is large enough. Indeed, it is well known that ideal kink instabilities can occur in line-tied coronal fields if the current density exceeds a critical threshold.^{10,26-29} In Sec. III we consider the relaxation of the coronal plasma in the event of such an instability if the resistivity is zero but the viscosity is nonzero and finite. The absence of resistivity keeps the footpoints frozen, but the total kinetic energy of the system can be gradually dissipated

by viscosity. Such a relaxation process has been invoked by Longcope and Strauss to argue that a second equilibrium must exist.⁵

III. MAGNETIC RELAXATION AND NONEQUILIBRIUM

Consider a static but unstable equilibrium of the RMHD equations (1) and (2) with zero η but nonzero ν , satisfying the equilibrium condition (3). A small perturbation can produce large flows (kinetic energy) which are then dissipated according to the energy equation,

$$\frac{dE}{dt} = \frac{d}{2dt} \left\{ \int (|\nabla_\perp A|^2 + |\nabla_\perp \phi|^2) d^3x \right\} = -\nu \int \Omega^2 d^3x. \quad (7)$$

The system must eventually relax to a state with lower energy such that

$$\int_0^\infty \frac{dE}{dt} dt = -\nu \int_0^\infty \left[\int \Omega^2 d^3x \right] dt = \text{const}, \quad (8)$$

which should be independent of the viscosity ν . To ensure this, we require that

$$\frac{dE}{dt}(t \rightarrow \infty) = -\nu \int \Omega^2(t \rightarrow \infty) d^3x \rightarrow 0. \quad (9)$$

One possibility, considered in Ref. 5, is that the system will relax to another static equilibrium with $\phi = \Omega = [\phi, \Omega] = \nabla_\perp^2 \Omega = 0$, satisfying Eq. (3). However, as demonstrated below by simple scaling arguments, it is also possible that the system can relax asymptotically to a nonequilibrium state with current sheet(s).

Assume that after a period of relaxation there is a current layer in the system with a typical width $\delta(t)$. [If the singularity occurs in infinite time, then $\delta(t \rightarrow \infty) \rightarrow 0$.] Let us consider the possibility of a nonequilibrium state which does not obey Eq. (3) everywhere. Assume that within the layer, the equation

$$\frac{\partial J}{\partial z} + [A, J] = O(\delta^{-\mu})$$

holds, where μ is a non-negative constant. To satisfy Eq. (1), we must have

$$\frac{\partial J}{\partial z} + [A, J] \sim -\nu \nabla_\perp^2 \Omega \sim O(\delta^{-\mu}). \quad (10)$$

We shall show, *a posteriori*, that the left-hand side of Eq. (1) is of lower order after we establish the range of μ . We now obtain $\nabla_\perp^2 \Omega \sim O(\delta^{-\mu}/\nu)$, or $\Omega \sim O(\delta^{2-\mu}/\nu)$. Substituting these orderings in Eq. (7) we obtain

$$\frac{dE}{dt} \sim O(\delta^{5-2\mu}/\nu). \quad (11)$$

To satisfy Eq. (9), μ must lie in the range

$$0 \leq \mu < 5/2, \quad (12)$$

which still leaves plenty of room for nonequilibrium with current sheet(s). For example, if $\mu=2$, we can have $\mathbf{B} \sim O(1)$, $J \sim O(\delta^{-1})$ without violating Eq. (10).

By Eq. (8), the energy difference between the initial and the final (asymptotic) state is

$$\Delta W = \int_0^\infty \frac{dE}{dt} dt \sim O\left[\frac{1}{\nu} \int_0^\infty \delta^{5-2\mu} dt\right] = \text{const}, \quad (13)$$

which should be finite (for $\mu < 5/2$) and independent of ν . This is ensured if the functional dependence of δ on ν can be written in the scale-invariant form $\delta(t) = \delta(t/\nu)$. Then increasing ν will slow down the rate of relaxation and decreasing ν will speed it up (which is indeed the general trend observed in the numerical simulations presented in Sec. IV). For example, if we assume that $\delta \sim \delta_0 \exp(-\lambda t/\nu)$ where $\lambda > 0$, we obtain $-\Delta W \sim \delta_0^{5-2\mu}/(5-2\mu)\lambda$ which is finite, positive in the range (12) and independent of ν . So it is possible, in principle, for the system to relax to a nonequilibrium state with current sheet(s), and at the same time satisfy the minimum-energy condition (9).

It is well known that the magnetic relaxation problem can be cast in the form of a variational principle.^{30,31} Consider the first variation of the energy integral for the RMHD equations:

$$\delta E = \int \nabla_\perp A \cdot \nabla_\perp \delta A d^3x = \int J \delta A d^3x. \quad (14)$$

Using Eq. (2) we can rewrite Eq. (14) in the form

$$\begin{aligned} \delta E &= \int J \left\{ \frac{\partial \phi}{\partial z} + [A, \phi] \right\} d^3x dt \\ &= - \int \phi \left\{ \frac{\partial J}{\partial z} + [A, J] \right\} d^3x dt, \end{aligned} \quad (15)$$

which vanishes for a minimum-energy state. Equation (15) implies that a stable static equilibrium satisfying Eq. (3) must be a minimum of the energy functional. However, *the converse may not be true*. If the system contains current sheet(s) and condition (12) applies, it follows from Eq. (10) that $\phi \sim O(\delta^{4-\mu})$ and $\delta E \sim O(\delta^{5-2\mu}) \rightarrow 0$. We thus conclude that although a minimum of the energy functional exists, the function that minimizes the functional may not. As is well-known in the theory of partial differential equations (cf. Ref. 32), such a solution is called a ‘‘weak’’ solution to distinguish it from a ‘‘strong’’ solution which satisfies Eq. (3) everywhere (as well as the specified boundary conditions).

The magnetic relaxation method indicates two possibilities for the (asymptotic) final state: a smooth equilibrium or nonequilibrium with current sheet(s). Which of these two possibilities is realized in Parker’s model? To answer this question, we present the following theorem in ideal RMHD with periodic boundary conditions in \mathbf{x}_\perp :

For any given footpoint mapping connected smoothly with the identity mapping $\mathbf{x}_\perp(L) = \mathbf{X}[\mathbf{x}_\perp(0), L] = \mathbf{x}_\perp(0)$, there is at most one smooth equilibrium.

The proof of this theorem, which uses the method of *reductio ad absurdum*, is given in Appendixes B and C. In constructing this proof, we assume that there exists a second smooth and stable equilibrium (of minimum energy), and show that this assumption leads to a contradiction.

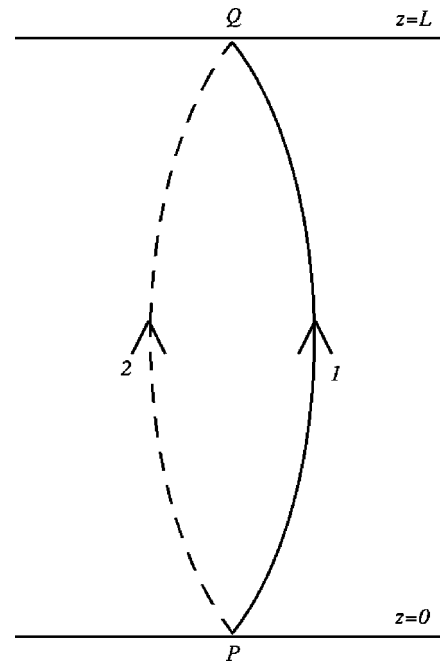


FIG. 1. Two field lines 1 and 2 connecting two points P and Q from $z = 0$ to $z = L$ on either side of a simple current sheet on the plane of the page.

The theorem implies that if a given stable magnetostatic equilibrium is driven by footpoint motions to evolve through a sequence of equilibria until it becomes unstable, there is no other smooth equilibrium for the unstable equilibrium to relax to. Then the unstable smooth equilibrium must relax to a nonequilibrium state with current sheet(s) (possibly as $t \rightarrow \infty$ if a finite-time singularity does not occur).

The theorem says nothing about the topology of the current sheet or about the time required to realize the singularity. VB has argued that the attainment of such a singular state is impossible by smooth footpoint motions because a current sheet in a magnetostatic equilibrium must involve a discontinuous footpoint mapping.² Variants of VB’s argument have appeared in the literature in recent years.^{5,33} In Ref. 33, it is proved that ‘‘simple’’ current sheets do not exist in Parker’s model, but the authors do add the caveat that their proof does not hold for current sheets of ‘‘arbitrarily complicated geometries.’’ They then suggest that such complicated geometries are ‘‘pathological’’ and unlikely to occur. We show below that the assumption of ‘‘simple’’ current sheets is over-restrictive, and excludes current sheets of great physical interest that are neither arbitrarily complicated nor pathological. (Parker has made this point on a number of occasions by means of the ‘‘optical analogy.’’ See, for instance, p. 200 as well as other references cited in Chaps. 7 and 8 of Ref. 8. See also the review by Low.⁶)

We first review a variant of VB’s argument discussed in Ref. 33. (Their proof is based on force-free MHD rather than RMHD, but this difference is not germane to our discussion.) Let us assume, as in Fig. 1, that there is a current sheet on the plane of the page. Let \mathbf{B}_1 be the magnetic field on the top of the sheet, and \mathbf{B}_2 the field on the bottom. Note that, for a force-free MHD equilibrium, the current density \mathbf{J} follows the direction of the magnetic field. Consider a point P on the

current sheet at $z=0$. On the top of the sheet, a magnetic field line starting from a point infinitesimally close to P connects to a point at $z=L$ infinitesimally close to a point Q on the current sheet. Label this field line 1. Consider another field line 2 which connects points infinitesimally close to P and Q on the bottom of the sheet. Since the footpoint motions on the boundary are smooth, field lines 1 and 2 connect points that are infinitesimally close initially at $z=0$ and $z=L$, and continue to be so for all times. Since the current flows entirely along the current sheet and never leaves it, the current path on a finite and singly connected sheet must close.³³ Hence $\oint \mathbf{B} \cdot d\mathbf{l} = 0$ for any loop that lies on top or on the bottom of the sheet (but does not cross the sheet). We now take a path integral around a closed loop on the top of the sheet extending from P to Q along 1 and from Q to P along 2 (although the magnetic field on top of the sheet is not parallel to the path 2). We obtain

$$\oint \mathbf{B} \cdot d\mathbf{l} = \int_1 B_1(l) dl - \int_2 \mathbf{B}_1(l) \cdot \hat{\mathbf{B}}_2(l) dl = 0, \quad (16)$$

where $\hat{\mathbf{B}}$ is the unit vector in the direction of the magnetic field. Similarly, the path on the bottom of the sheet extending from P to Q along 2 and back to P along 1, yields

$$\oint \mathbf{B} \cdot d\mathbf{l} = \int_2 B_2(l) dl - \int_1 \mathbf{B}_2(l) \cdot \hat{\mathbf{B}}_1(l) dl = 0. \quad (17)$$

Since the magnitude of the magnetic field is continuous across the current sheet, that is, $B_1(l) = B_2(l) \equiv B(l)$, we add Eqs. (16) and (17) to obtain

$$\int_{1+2} B(l) [1 - \hat{\mathbf{B}}_2(l) \cdot \hat{\mathbf{B}}_1(l)] dl = 0. \quad (18)$$

Since the integrand on the left-hand side of Eq. (18) is always positive, the integrand itself must vanish in order for the integral to vanish, which implies that there cannot be a net current inside the sheet.

The validity of the argument given above relies on strong assumptions regarding the geometry of the current sheet. We demonstrate below that the argument fails for a current sheet with a geometry less trivial than the simple geometry imagined in Fig. 1. In Fig. 2 we show schematically a current sheet of the Y type in which two branches of the sheet are joined along the line IJ . The field line 1 on the top of the front sheet intersects the line IJ , while the field line 2 on the bottom with end points infinitesimally close to P and Q remains to the left of that line and does not cut through it. Now, although Eq. (16) still holds, Eq. (17) does not since the loop on the bottom will cut through the current sheet and thus allow a net current to flow through the loop. Therefore, Eq. (18) does not apply and the magnetic field can change direction across the current sheet, allowing a net current inside.

The current sheet topology shown in Fig. 2 is a three-dimensional generalization of the current sheet spanning Y points commonly seen in two-dimensional (2-D) MHD. For instance, during the nonlinear evolution of the ideal coalescence instability, the X -point structure in the initial stage of island coalescence can evolve into a structure of the type

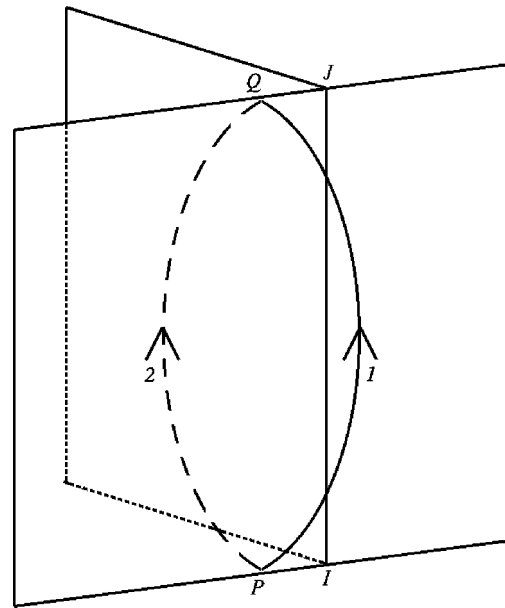


FIG. 2. Two current sheets making contact along the line IJ , with two field lines similar to those in Fig. 1 on either side of the front sheet. Note that only line 1 crosses IJ .

shown in Fig. 3. The two separatrices $ABCD$ and $EFGH$ make contact with each other over a surface (referred to as the contact surface) bounded by the two curves connecting points I and J . Following through with the argument given in the last paragraph, we can show by considering field lines 1 and 2 between the points P and Q that Eq. (18) does not hold. Note that field lines near the point I along EH diverge along the line FG , and field lines along AB converge near the point J . Therefore the region of strong current density which lies along AB on the $z=0$ plane, turns as z increases

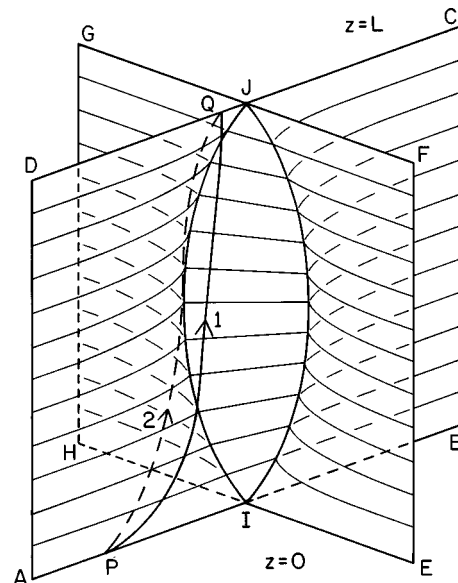


FIG. 3. Two separatrices $ABCD$ and $EFGH$ make contact with each other over a surface bounded by two curves connecting the two end points I and J . This contact surface is in alignment with the line AB near $z=0$, and with the line FG near $z=L$ so that its orientation is twisted by $\pi/2$ along z . Two field lines similar to those in Fig. 2 are shown on the sheet $AIJD$.

and lies along FG on the $z=L$ plane. Thus the contact surface is aligned with the line AB near the point I , and with the line FG near the point J . This is a feature seen in the numerical simulations discussed in Sec. IV.

The tendency of the system to evolve to a singular non-equilibrium state suggests that the ‘‘fields are condemned, like Sisyphus, to an ‘eternity’ of activity.’’³⁴ This interesting analogy appears to contradict our physical intuition that the system should somehow eventually relax to a smooth equilibrium. We remark that the seeming inability of the system to find a smooth relaxed state is a consequence of constraining the dynamics by the ideal MHD equations for all times. Inevitably, as the current sheet becomes very intense, the $\eta \nabla_{\perp}^2 A$ term will become comparable to other terms in Eq. (2) for even very small but nonzero values of η . If this occurs at time $\tau(\eta)$ [where $\tau(\eta \rightarrow 0) \rightarrow \infty$ for an infinite-time singularity], slippage due to resistivity will intercede and reconnection will take place. Then magnetic field lines can be broken and the footpoint mapping can change without any motion of footpoints on the boundary. In the limit $\eta \rightarrow 0$, the current layers will grow increasingly singular due to helicity-conserving reconnection^{35,36} but preserve the smoothness of the footpoint mapping, as suggested in Ref. 36. Eventually, the footpoint mapping will be simplified sufficiently by reconnection, so that the active system can relax to a stable and quiescent equilibrium. (It can then escape the mythical curse of Sisyphus to find rest, albeit short-lived.) The cycle of footpoint motions and strong current intensification can then be repeated all over again.

IV. NUMERICAL SIMULATIONS

We have carried out some numerical simulations of Parker’s model using the RMHD equations (1) and (2), with periodic boundary conditions in \mathbf{x}_{\perp} . The latter enable us to use a pseudospectral method. We impose line-tied boundary condition on the $z=0, L$ planes and use a finite difference scheme along z . For comparison, we also present some 2-D examples, obtained by taking the $L \rightarrow \infty$ limit of three-dimensional (3-D) cases. The highest numerical resolution is 256×256 for 2-D cases, and $64 \times 64 \times 16$ for 3-D cases. As estimated in Ref. 5 and discussed in Sec. I, it is extremely difficult to distinguish between a truly singular nonequilibrium and a smooth equilibrium with very thin current layers, especially at this level of spatial resolution. However, such simulations are still useful because they help establish some qualitative trends of the dynamics in the low-dissipation limit.

We first report the results of computer runs for the ideal coalescence instability in 2-D as well as in 3-D line-tied geometry. The initial condition is^{14,37}

$$A_0(x, y) = \bar{A} \sin(2\pi x) \sin(2\pi y), \quad (19)$$

with B_z equal to unity. For the 2-D MHD equations, that is, Eqs. (1) and (2) with $\partial/\partial z = 0$, it has been shown³⁷ that the static equilibrium (19) is always unstable to the ideal coalescence instability. In an ideal plasma, as the two islands tend to merge, the initial angle (with respect to y) between two separatrices that intersect at the X point tends to decrease

sharply, and a current sheet spanning Y point tends to form in an ideal saturated state. In practice, however, the effect of finite resistivity (either numerical or physical) causes magnetic reconnection, and the two islands coalesce to form one.

Unlike the 2-D case, the 3-D line-tied case with the initial state prescribed by Eq. (19) is not always unstable. When deformed by a constant footpoint drive [Appendix A, Eq. (A3)], the condition for instability is $4\pi^2 \bar{A} L > 10.81$.^{5,14} After an instability is triggered, the dynamical evolution of A exhibits strong z dependence. By examining the projection of the level surfaces of A near $z=L/2$, we find that this middle region evolves in a manner very similar to the 2-D case. This is not surprising since near $z=L/2$ the $\partial/\partial z$ terms in Eqs. (1) and (2) are very small. By simple order-of-magnitude estimates, with $\partial/\partial z \sim 1/L$, $\nabla_{\perp} \sim \kappa$, $A \sim \bar{A}$ and $\phi \sim \bar{\phi}$, we find that the condition

$$\kappa^2 \bar{A} L \gg 1 \quad (20)$$

can be easily satisfied when the instability condition $4\pi^2 \bar{A} L > 10.81$ holds. Under these conditions, the system will tend to be weakly z dependent in the middle region and show a pronounced tendency, as in 2-D, to develop current sheets. However, near the two end plates, the dynamics is qualitatively different from that in the middle region. In particular, the $\partial/\partial z$ terms tend to be much larger at the plates due to the imposed boundary conditions. Thus the current layer that develops in the aftermath of the instability violates Eq. (3) and is neither in equilibrium nor appears to be tending towards one.

Current layers can, of course, form in Parker’s model without the mediation of the coalescence instability. Such layer structures have been seen in a number of simulations.^{38–40} In our own 3-D RMHD simulations, such current layers can be easily obtained by applying constant footpoint motions prescribed by the stream functions $\phi(\mathbf{x}_{\perp}, 0) = 0$, $\phi(\mathbf{x}_{\perp}, L) = \phi_0(\mathbf{x}_{\perp})$ which do not satisfy the condition $[\phi_0, \nabla_{\perp}^2 \phi_0] = 0$ and are small enough that the system has time to relax to a quasiequilibrium state during the footpoint motions. Figure 4 shows the contours of current density J for $z=0, L/4, L/2, L$ after a period $t=t_1 \approx 118.5$ with a constant footpoint drive (with root mean square velocity ≈ 0.00494 on $z=L$). In these simulations, the viscosity ν is chosen to be $\nu=0.01$ and the resistivity η is set to zero; however, numerical resistivity is unavoidable due to the finite size of the spatial grid. In Fig. 4 we can identify two principal current layers in the periodic simulation box. The maximum and minimum values of J in the four cross-sections (a)–(d) are roughly the same, indicating that the system satisfies Eq. (3) and is nearly in equilibrium. The footpoint mapping at the same instant of time is shown in Fig. 5(a)[5(d)], showing the deformation of the grid at $z=0$ [$z=L$] from an initial, equally spaced square grid at $z=L$ [$z=0$]. The mapping obtained from Eqs. (4) and (5) at $z=L/4$ and $z=L/2$ are also shown in Figs. 5(b) and 5(c), respectively. Note that the current layers tend to occur at the sites where the mapping is most severely distorted.

We focus on the equilibrium in Fig. 4 because it is roughly at marginal ideal stability. (We say roughly because

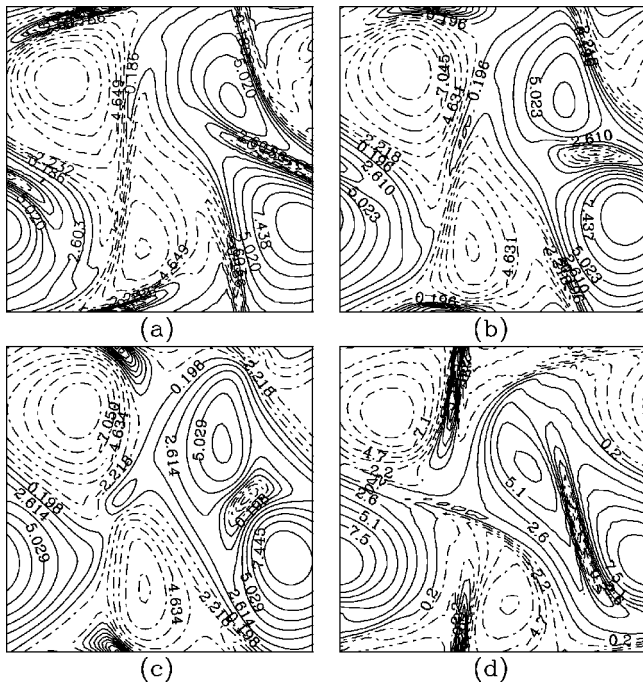


FIG. 4. Contour plots of current density J for 2-D cross sections at (a) $z=0$, (b) $z=L/4$, (c) $z=L/2$ and (d) $z=L$, after a period $t=118.5$ of constant footpoint drive. Maximum and minimum current density are $J_{\max} \approx 9.9$ and $J_{\min} \approx -9.5$ for all z .

it is difficult to determine sharply a marginally stable equilibrium in a numerical experiment.) An equilibrium obtained from the same footpoint motion for $t < t_1 \approx 118.5$ can be shown to be stable by the magnetic relaxation method. This is done numerically by setting $\phi(\mathbf{x})=0$ instantaneously at the end of short intervals of time during the entire relaxation process [keeping the boundary condition $\phi(z=0, L)=0$ fixed]. The equilibrium is seen to relax to a state very close to the initial state, indicating that the initial state is a stable equilibrium.

In contrast, we find it is much more difficult to obtain such equilibria for $t > t_1 \approx 118.5$. In this case the current density near $z=L/2$ increases faster with time than it does near $z=0, L$, which we interpret as signatures of nonequilibrium. In Table I we present numerical evidence in support of this interpretation. We show that as t increases, the maximum of the current density J_{\max} over the whole space (second column) becomes increasingly larger than $J_{\max 0}$, the maximum current density over the $z=0$ plane (third column). (If the system were approaching equilibrium, J_{\max} and $J_{\max 0}$ would tend to be the same.) We also quantify the departure from

TABLE I. Some values of J_{\max} , $J_{\max 0}$, $\langle q^2 \rangle$, $\langle d^2 \rangle$, q_{\max} and d_{\max} at four instants of time beyond the threshold of marginal stability in the numerical simulation.

t	J_{\max}	$J_{\max 0}$	$\langle q^2 \rangle$	$\langle d^2 \rangle$	q_{\max}	d_{\max}
118.5	9.9073	9.8551	0.2326	0.000 279	7.946	0.7084
131.6	16.477	10.855	0.9302	0.002 377	16.04	2.2722
145.6	28.278	14.621	4.3611	0.1471	32.937	5.9972
150.5	35.265	16.41	21.984	13.486	83.387	79.009

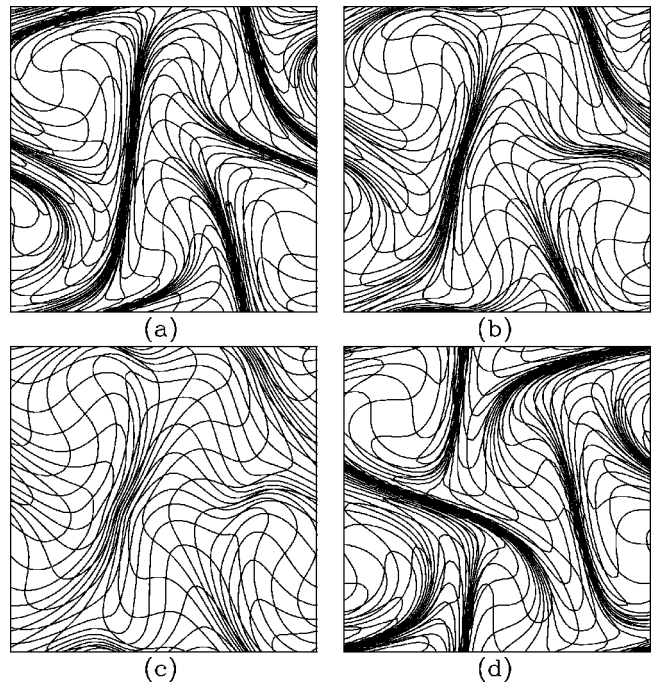


FIG. 5. Footpoint mappings at the same cross sections and the same time as in Fig. 4, showing that the current layers of Fig. 4 are located where the mapping is most distorted.

equilibrium by calculating the quantity $q \equiv \partial J / \partial z + [A, J]$. In particular, $\langle q^2 \rangle$ (fourth column) denotes the integrated average of q^2 over a unit cell and q_{\max} (sixth column) denotes its maximum magnitude over space. The values of both these quantities at four instants of time are shown in Table I, and exhibit a clear trend of increasing departure from equilibrium (that is, $q=0$) for $t > t_1 \approx 118.5$. Also shown in Table I are the mean square (fifth column) and maximum values of the quantity $d \equiv q + \nu \nabla_{\perp}^2 \Omega$. The two terms on the right-hand side of d tend to cancel each other (except at the time $t=150.5$ when a numerical instability develops and invalidates the simulation). This cancellation is consistent with Eq. (10).

The observed numerical trends suggest that when the equilibrium becomes unstable, the system does not tend to a second magnetostatic equilibrium by relaxation. In Fig. 6 we show the contour plots of J at $t=150.5$. If we induce magnetic relaxation on any intermediate state within the time-interval separating Figs. 4 and 6, we find that the current layers become progressively thinner without showing any tendency of reaching a saturated width. (Qualitatively similar numerical results have been reported recently in Ref. 17.) For longer times, the instability is so strong that the localized vortical flows grow to large values in a short time, and even the exercise of setting $\phi(\mathbf{x})=0$ repeatedly at frequent intervals of time does not appear to move the system in the direction of an equilibrium. Eventually the current layers become so thin that they cannot be resolved numerically and the run terminates with a numerical instability.

It is our interpretation that similar physical instabilities are also present in the simulations⁴⁰ obtained by random footpoint motions. The current layers in Ref. 40 do not ap-

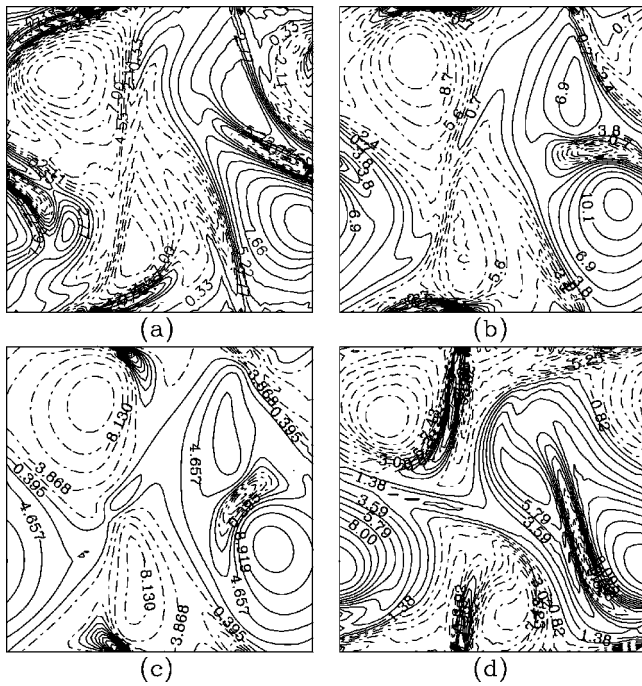


FIG. 6. Contour plots of current density J for cross sections at (a) $z=0$ with $J_{\max} \approx 16.4$, $J_{\min} \approx -12.3$, (b) $z=L/4$ with $J_{\max} \approx 25.4$, $J_{\min} \approx -15.1$, (c) $z=L/2$ with $J_{\max} \approx 34.5$, $J_{\min} \approx -15.7$ and (d) $z=L$ with $J_{\max} \approx 15.7$, $J_{\min} \approx -11.9$, showing nonequilibrium with stronger current layers than those in Fig. 4, after a period $t=150.5$ of constant footpoint drive.

pear to be in equilibrium, since the current density is much stronger near $z=L/2$ than it is near $z=0, L$.

In summary, we find by numerical simulation that current layers can be realized in a stable equilibrium easily by steady or random footpoint motions. However, such current layers can be driven unstable if the footpoint motions exceed a threshold. When that occurs, it appears impossible to attain a second magnetostatic equilibrium, and the current layers continue to grow more intense and thinner until we reach the limit of spatial resolution in our computations. We suggest that the system approaches nonequilibrium with current sheet(s), consistent with our analytical results in Sec. III. Due to limitations of numerical resolution, we cannot provide conclusive evidence that the scaling of terms, prescribed by Eq. (10), is indeed satisfied in our simulations.

V. 3-D CURRENT SHEETS WITHOUT NULLS OR CLOSED FIELD LINES

It is well known that current sheets can occur in systems with easily identifiable magnetic separatrices such as closed field lines, nulls or X-type neutral lines. (See, for instance, Ref. 41 and other references therein.) One of the challenges posed by Parker's model is that it does not have such easily identifiable separatrices. Yet the analytical and computational results presented above demonstrate that nonequilibrium with current sheets can and do occur in Parker's model. What criterion should we use to track the current sheets in models (such as Parker's) where field lines have finite length, do not close on themselves and do not appear to develop nulls? The answer to this question has significant

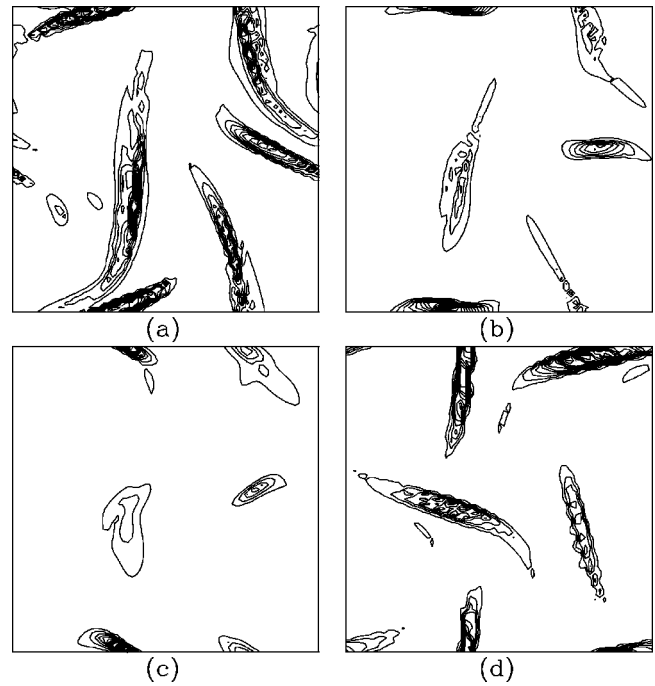


FIG. 7. Contour plots of $\lambda(x,y,z)$ (see text for definition) for cross sections at (a) $z=0$, (b) $z=L/4$, (c) $z=L/2$ and (d) $z=L$ at the same time as Fig. 6, showing the location of the region of velocity amplification which is largest where the current layers are strongest.

implications for the geometry and dynamics of magnetic reconnection in 3-D astrophysical plasmas.⁴²⁻⁴⁶

For an ideal fluid, we define the field line velocity $\mathbf{v} = \nabla \Phi \times \mathbf{B}/B^2$ for a scalar function Φ which is constant along a magnetic field, that is, $\mathbf{B} \cdot \nabla \Phi = 0$. Following Greene,²³ we define the rate λ of amplification of the velocity by the relation

$$\lambda = \frac{1}{2B} \mathbf{B} \cdot \nabla \ln(Bv^2) = \frac{1}{2B} \mathbf{B} \cdot \nabla \ln(|\nabla \Phi|^2/B). \quad (21)$$

The advantage of this definition is that it mimics the concept of the Lyapunov exponent in nonlinear dynamics, and can be useful for systems in which field lines have finite length. Note that λ tends to infinity at magnetic nulls, but as we show below, that is not the only way that λ can become singular.

The inverse of any of the two mapping functions $X(\mathbf{x}_\perp, z)$ and $Y(\mathbf{x}_\perp, z)$, or a suitable combination of both, can be chosen to be the function Φ . In Fig. 7 we show contours of λ for the state depicted in Fig. 6. [These contours are generated from the root mean square of $X(\mathbf{x}_\perp, z)$ and $Y(\mathbf{x}_\perp, z)$.] Note that λ can become extremely large if the mapping becomes very distorted. It is clear by inspection of Figs. 6 and 7 that the regions of strong current density are tracked reasonably well by the contours of λ . The velocity amplification is large in these regions, suggesting that they are the likely sites for the onset of reconnection. We note, however, that not all regions of high λ (or high distortions of the mapping) are necessarily regions of high current density (as can be seen, for instance, by a close comparison of Figs. 6(d) and 7(d) [or 5(d)]). Two families of neighboring field

lines, pointing in the same direction but diverging away from each other can contribute, for geometrical reasons, to a strong distortion of the mapping, but they do not necessarily create regions where the current density is high or field lines can reconnect. In view of this, we suggest that the unbounded growth of λ is a necessary but not a sufficient condition for current singularities.

VI. CONCLUSION

Based on the RMHD equations in the ideal limit, we have shown that in Parker's model of the solar corona, there is at most one smooth equilibrium for each smooth footpoint mapping. A smooth stable equilibrium may remain smooth but become unstable when driven by footpoint motions beyond a critical threshold. When that occurs, there is no second smooth equilibrium that the system can relax to. Instead, the system must relax to a nonequilibrium state with current sheet(s) (although it may take the system infinite time to do so). We have also shown that such a nonequilibrium state may indeed be a minimum-energy state, accessible by magnetic relaxation. We have considered the topological structure of such current sheets, and shown that they are not subject to the constraints discussed by van Ballegooijen.²

We have relied on the reduced ideal MHD equations and periodic boundary conditions to construct a proof of the theorem stated in Sec. III (and proved in Appendixes B and C). We do not know if the theorem can be proved for the full MHD equations, but suspect that it will hold. The numerical results presented in Ref. 17 do not rely on RMHD ordering, but the qualitative conclusions are similar.

We have carried out some numerical simulations to test the principal theoretical conclusions arrived at in this paper. Although it is difficult to distinguish a true current singularity from a very thin but smooth current layer in numerical simulations, we do observe that an unstable current layer shows a tendency to evolve towards a nonequilibrium state with the current density growing much faster in the middle region than near the two end plates. While limitations of spatial resolution do not allow us to obtain a specific scaling for the current sheet, we give some quantitative evidence indicating a clear trend towards nonequilibrium.

Finally, it is suggested that in 3-D plasmas without closed field lines or nulls, a necessary condition determining the sites of current sheets is where the rate of velocity amplification, defined by Eq. (21), becomes arbitrarily large in the ideal limit.

ACKNOWLEDGMENTS

This research was supported by the National Science Foundation Grant No. ATM 93-10157 and National Aeronautics and Space Administration Grant No. NAG5-3716. Supercomputing resources were provided by the San Diego Supercomputer Center.

APPENDIX A: SOME PROPERTIES OF THE VAN BALLEGOOIJEN EQUATION

We discuss the existence and uniqueness of solutions of the van Ballegooijen (VB) equation (6) which, with appropriate boundary conditions, represents a two-point boundary-value problem. These considerations are useful in our demonstration of the theorem stated in Sec. III. Note that the theorem is concerned with the uniqueness of a smooth equilibrium solution, given a smooth footpoint mapping. Although the VB equation is used in our proof of this theorem, the theorem neither assumes nor requires that the solution of the VB equation be unique. In this section we discuss some basic criteria for the existence and uniqueness (or nonuniqueness) of solutions of the VB equation.

To be specific, we assume periodic boundary condition in \mathbf{x}_\perp . Then, ϕ and A can be written as

$$\phi(\mathbf{x}, t) = \sum_{lm} \phi_{lm}(z, t) e^{2\pi i(lx + my)}, \quad (\text{A1})$$

$$A(\mathbf{x}, t) = \sum_{lm} A_{lm}(z, t) e^{2\pi i(lx + my)},$$

where we have chosen the periods to be unity in both directions, x and y , without loss of generality. Note that this periodicity in Eq. (A1) is preserved by (1) and (2) for all times if the initial condition is periodic. If ϕ and A are smooth functions, the sums in (A1) converge and can be approximated, for any specified accuracy, by a finite number of terms in the series. Using the Fourier components in Eq. (A1), we can formally rewrite the VB equation (6) (at a given time) as an infinite set of linear ordinary differential equations (ODEs),

$$\phi''_\alpha + H_{\alpha\beta}(z) \phi'_\beta + K_{\alpha\beta}(z) \phi_\beta = 0, \quad (\text{A2})$$

subject to the boundary conditions $\phi_\alpha(0)$ and $\phi_\alpha(L)$, where α or β indicates one Fourier index (l, m), $H_{\alpha\beta}(z)$ and $K_{\alpha\beta}(z)$ are matrices that depend on the given equilibrium A , and the prime denotes derivative with respect to z .

Although Eq. (A2) comprises an infinite set of ordinary differential equations (ODEs), the solution can be approximated up to any specified accuracy by a finite number of equations if ϕ and A are assumed smooth. We can then invoke some mathematically rigorous results about boundary-value problems involving a finite set of ODEs (cf. Ref. 47). In general, a solution of Eq. (A2) can be shown to exist, but whether it is unique or not depends on the matrices $H_{\alpha\beta}$ and $K_{\alpha\beta}$. If a solution is not unique, there must be a nontrivial solution $\tilde{\phi}_\alpha$ of Eq. (A2) satisfying the boundary conditions $\tilde{\phi}_\alpha(0) = \tilde{\phi}_\alpha(L) = 0$. The existence of such a nontrivial solution is sufficient to make the solution nonunique: if ϕ_α is a solution of Eq. (A2) for the specified boundary condition, so is $\phi_\alpha + c\tilde{\phi}_\alpha$ where c is an arbitrary constant. Since the two matrices $H_{\alpha\beta}$ and $K_{\alpha\beta}$ are, in general, difficult to evaluate and are actually part of the solution to the problem (for given footpoint motion), it is difficult to settle the question of uniqueness *a priori*. However, in the simple case $A=0$ (uni-

form magnetic field), the VB equation reduces to $\partial^2 \Omega / \partial z^2 = 0$ which has a unique solution, $[\phi(L) - \phi(0)]z/L + \phi(0)$, for any given $\phi(0)$ and $\phi(L)$.

The existence of smooth solutions of the VB equation implies that a smooth equilibrium $A(x, y, z, t)$ can always be found for any footpoint motion. For example, if the footpoint motion

$$\phi(\mathbf{x}_\perp, 0, t) = 0, \quad \phi(\mathbf{x}_\perp, L, t) = \phi_e(\mathbf{x}_\perp)L, \quad (A3)$$

where $[\phi_e, \nabla_\perp^2 \phi_e] = 0$ is applied to a uniform magnetic field which produces the identity mapping $\mathbf{x}_\perp(L) = \mathbf{x}_\perp(0)$, a solution of the VB equation is

$$\phi(\mathbf{x}, t) = \phi_e z, \quad A(\mathbf{x}, t) = \phi_e t. \quad (A4)$$

Note that a solution can be found for the VB equation even if the equilibrium is unstable. The line-tied coalescence instability,^{5,14} provides an example. When the footpoint motion $\phi_e = \sin(2\pi x)\sin(2\pi y)$ is applied, instability sets in when $4\pi^2 tL > 10.81$, but the occurrence of the instability does not preclude the existence of smooth (but unstable) equilibrium solutions of the VB equation even for $t > 10.81/4\pi^2 L$.

Any smooth equilibrium $\tilde{A}(\mathbf{x}_\perp, z)$ satisfying Eq. (3) can be produced, starting with $A = 0$, by applying the following footpoint drive

$$\phi(\mathbf{x}_\perp, 0, t) = 0, \quad \phi(\mathbf{x}_\perp, L, t) = \tilde{A}(\mathbf{x}_\perp, Lt)L. \quad (A5)$$

A smooth solution of the VB equation for the footpoint drive (A5) is given by

$$\phi(\mathbf{x}_\perp, z, t) = \tilde{A}(\mathbf{x}_\perp, z)t, \quad A(\mathbf{x}_\perp, z, t) = \tilde{A}(\mathbf{x}_\perp, z)t, \quad (A6)$$

which gives $A = \tilde{A}$ at $t = 1$. Note that Eqs. (A3) and (A4) are special cases of Eqs. (A5) and (A6).

APPENDIX B: EXISTENCE OF AT MOST ONE SMOOTH EQUILIBRIUM FOR EACH FOOTPOINT MAPPING

Before we discuss the proof of the theorem stated in Sec. III, we make three (provable) assertions about solutions of the VB equation (6). Since these assertions are used extensively in the proof that follows, we write them down at the outset for ease of reference.

Assertion (i): *Any smooth equilibrium can be constructed by solving the VB equation, beginning from a uniform magnetic field and applying smooth footpoint motions.*

This assertion can be proved by referring to Appendix A, where we note that any smooth equilibrium $A = \tilde{A}(\mathbf{x}_\perp, z)$ can be produced by solving the VB equation starting from a uniform magnetic field and applying the footpoint drive (A5).

Assertion (ii): *Any solution of the VB equation, so constructed, is reversible.*

It is easy to show that if we apply the footpoint drive (A5) on solution (A6) in reverse time from $t = 1$ to $t = 0$, the equilibrium $A = \tilde{A}(\mathbf{x}_\perp, z)$ will return to a uniform magnetic field.

Assertion (iii): *Any solution of the VB equation, constructed from a smooth equilibrium with a smooth footpoint drive, is smooth.*

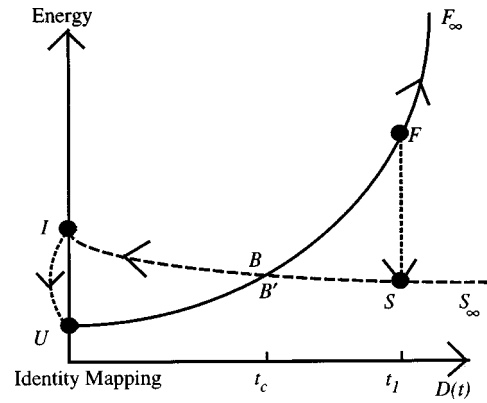


FIG. 8. Schematic diagram for the proof of the theorem (Appendix B) that there is at most one equilibrium for a given smooth footpoint mapping.

The reader is referred to Ref. 2 for a proof of this assertion.

We now give a proof of the theorem stated in Sec. III. The proof uses the method of *reductio ad absurdum*. The argument is developed in six steps which can be understood by referring to the schematic diagram in Fig. 8:

- (1) Start (at $t = 0$) with an equilibrium U which contains a uniform magnetic field and yields the identity mapping.
- (2) Obtain a smooth, unstable equilibrium F , with $A = \tilde{A}(\mathbf{x}_\perp, z)$, by imposing a smooth footpoint drive $D(t)$ from $t = 0$ to $t = t_1 = 1$. The passage from U to F occurs through a sequence of smooth equilibria [assertion (i)] represented by the curve UBF , where the point B represents a marginally stable equilibrium, obtained at $t = t_c$.
- (3) Assume that F relax to a second smooth state S with the same footpoint mapping as F .
- (4) Apply $D(t)$ on S in reverse time from $t = t_1$ to $t = t_c$. The system will follow the path SB' which represents a sequence of smooth stable equilibria. (Note that in Fig. 8, which is a two-dimensional schematic representation of an infinite-dimensional space, the point B lies on the path marked by the solid line, whereas B' lies on the path marked by the dotted line.) That this can be done is shown as follows.

The footpoint drive $D(t)$ can be applied to U to generate not only the smooth (but unstable) equilibrium F [assertion (i)], but if applied continuously for infinite time, it can also generate a sequence of smooth (but increasingly unstable) equilibria along the curve FF_∞ . This sequence of unstable equilibria must then relax to the curve SS_∞ which, by assumption (3), represents smooth and stable equilibria. By continuity, we should also be able to produce the same branch SS_∞ by solving the VB equation starting with the equilibrium S and applying the footpoint drive $D(t)$. It follows that we can apply $D(t)$ on S in reverse time [assertion (ii)] from $t = t_1$ to $t = t_c$ to produce the branch SB' of smooth and stable equilibria.

- (5) Continue further application of $D(t)$ in reverse time along SB' . The path taken by the system depends, in principle, on two possibilities: (a) either the VB equation

has a unique solution for all times or (b) the solution becomes nonunique at one (or more) point(s) along the reversal path.

If (a) is true, the system must follow a path $B'I$, distinct from the path BU , and attain at $t=0$ the smooth equilibrium I , described by the identity mapping. Since the initial state U is also described by the identity mapping, there must exist more than one smooth equilibrium for the identity mapping. We show below [after step (6)] that this contradicts the result proved in Appendix C. Hence the continuous curve $SB'I$ cannot exist, and application of the footpoint drive $D(t)$ in reverse time on S must bring it back to the state U along some path. This path must then intersect the original path UB at some point. We make the natural assumption that this point of intersection is the marginal equilibrium point B (which now coalesces with the point B'). The solution of the VB equation must be nonunique at the point B , which requires us to consider possibility (b).

In case (b), application of the footpoint drive $D(t)$ at b in reverse time for $-t_c$ will bring the footpoint mapping back to the identity mapping. Using continuous footpoint motions, we show below [after step (6)] that we can then obtain an infinite sequence of equilibria, including one that is infinitesimally close to U . Furthermore, although this infinite sequence of equilibria correspond to the identity mapping, they are all distinct from the state U which is a uniform magnetic field. Once again, the result proved in Appendix C yields a contradiction because an equilibrium that corresponds to the identity mapping and is infinitesimally close to the uniform magnetic field cannot be smooth.

(6) The contradiction obtained in step (5) shows that assumption (3) cannot be sustained. In other words, the second equilibrium S cannot be assumed to be smooth. Hence there is at most one smooth equilibrium for a given smooth footpoint mapping.

The contradiction of assumption (3) is key to this proof. We discuss below this contradiction in more detail.

As discussed in step (5), when we apply $D(t)$ in reverse time along the branch SB' , there are two possibilities:

(a) *The VB equation has a unique solution*

This implies that the VB equation has a unique solution at every step of the reversal path. We apply the footpoint drive $D(t)$ in reverse time on S along the curve $SB'I$ back to an equilibrium I with an identity mapping. Note that I cannot equal U because the uniqueness assumption precludes it. Therefore there must exist another smooth equilibrium I with $A=A_0 \neq 0$ for the identity mapping. We now show that this cannot be.

If A_0 exists, $A_0(x, y, z)$ must be periodic in z with period L . Since we also assume periodic boundary condition in \mathbf{x}_\perp , we can write

$$A_0(x, y, z) = \sum_{lmn} A_{lmn} e^{2\pi i(lx + my + nz/L)}, \quad (\text{B1})$$

where A_{lmn} are constants. Note that $nA_0[m(x-\bar{x}), m(y-\bar{y}), n(z-\bar{z})]/m^2$ is also an equilibrium solution for the identity mapping between $z=0$ and L for any integers n, m

and constants $\bar{x}, \bar{y}, \bar{z}$. Application of the footpoint drive $D(t)$ on these equilibria from $t=0$ to t_1 will produce a continuum of equilibria at $t=t_1$, all of which correspond to the same footpoint mapping as F and S . This, in turn, implies that the solution of the VB equation for A_0 is not unique which contradicts our assumption. To see this, let us solve the VB equation for A_0 , subject to the boundary conditions $\phi(0) = \phi(L) = 0$. The trivial solution is $\phi=0$. If there exist a nontrivial solution, then the solution is nonunique (Appendix A). Such a nontrivial solution ϕ must satisfy

$$\frac{\partial \phi}{\partial z} + [A_0, \phi] = c_x \frac{\partial A_0}{\partial x} + c_y \frac{\partial A_0}{\partial y} + c_z \frac{\partial A_0}{\partial z}, \quad (\text{B2})$$

for any constants c_x, c_y, c_z . Direct substitution of Eq. (B2) into the VB equation yields

$$\left(c_x \frac{\partial}{\partial x} + c_y \frac{\partial}{\partial y} + c_z \frac{\partial}{\partial z} \right) \left(\frac{\partial J_0}{\partial z} + [A_0, J_0] \right) = 0, \quad (\text{B3})$$

which ensures that any solution of Eq. (B2) must satisfy the VB equation. Since the solution A_0 yields the identity mapping, we can show that a solution to Eq. (B2) can always be found by writing $\phi_0 = \phi - c_y x + c_x y - c_z A_0$ where ϕ_0 satisfies the advection equation for a passive scalar,

$$\frac{\partial \phi_0}{\partial z} + [A_0, \phi_0] = 0, \quad (\text{B4})$$

$$\phi_0(\mathbf{x}_\perp, 0) = \phi_0(\mathbf{x}_\perp, L) = c_{xy} - c_{yx} - c_z A_0(\mathbf{x}_\perp, 0).$$

Note that every solution A_0 that corresponds to a nonuniform magnetic field and yields the identity mapping can be produced by applying the footpoint drive (A5) beginning with a uniform magnetic field [assertion (i)]. We can then apply the same footpoint drive in reverse on A_0 till we return to the uniform magnetic field and restore the footpoint mapping to the identity mapping [assertion (ii)]. However, the equilibrium we thus obtain will depend on the particular solution of ϕ we start with, and on the values of the constants c_x, c_y, c_z in Eq. (B2). In particular, when $c_i \rightarrow 0$, we should obtain a smooth equilibrium that is infinitesimally close to $A=0$ and satisfies the identity map by continuity because A_0 is assumed to be smooth, and the process of reversing the footpoint drive should be smooth as well [assertion (iii)]. The result proved in Appendix C now yields a contradiction. Therefore A_0 cannot be smooth. In other words, the assumption that there exists a smooth equilibrium $A_0 \neq 0$ satisfying the identity mapping is not valid. Hence the continuous curve $SB'I$ does not exist, and application of the footpoint drive $D(t)$ in reverse time on S must bring it back to the identity mapping (with uniform field U) along some path. This path must then intersect the original path UB at some point. Since the solution of the VB equation must be nonunique at that point, we are required to consider the following possibility.

(b) *The VB equation has a nonunique solution*

As discussed in step (5), we consider the situation when the marginally stable equilibrium B (realized at $t=t_c$) is the point of nonuniqueness. (Obviously $t_c \neq 0$ since at $t=0$, we

have $A=0$ which yields a unique solution of the VB equation.) Then, the application of $D(t)$ on S in reverse time will return S to U along the path SBU .

Now let ϕ_1 be the solution (at $t=t_c$) that leads to the branch BF , and ϕ_2 be another solution that leads to the branch BS . We can write

$$A_F(t_c + \delta t) \approx A(t_c) + \left\{ \frac{\partial \phi_1}{\partial z} + [A(t_c), \phi_1] \right\} \delta t,$$

$$A_S(t_c + \delta t) \approx A(t_c) + \left\{ \frac{\partial \phi_2}{\partial z} + [A(t_c), \phi_2] \right\} \delta t,$$

for a sufficiently small interval δt (which can be positive or negative). Then the difference $\Delta \phi = \phi_1 - \phi_2$ is a solution of the VB equation at $t=t_c$, satisfying the boundary condition $\phi(0) = \phi(L) = 0$. Furthermore, any function $\phi_c = \phi_1 + c \Delta \phi$ is also a solution, where c is an arbitrary constant. Hence we can write

$$A_c(t_c + \delta t) \approx A_F(t_c + \delta t) + c \left\{ \frac{\partial \Delta \phi}{\partial z} + [A(t_c), \Delta \phi] \right\} \delta t,$$

which is a smooth equilibrium for all values of c and for sufficiently small δt . Note that $A_c = A_F$ if and only if $c=0$. Similarly, $A_c = A_S$ if and only if $c=1$. Application of the footpoint drive $D(t)$ in reverse time for a time $-t_c$ will bring the footpoint mapping back to the identity mapping. Using a different ϕ_c as the initial solution, we can obtain a continuum of smooth equilibria $A_c(t)$ [assertion (iii)], with all $A_c(0)$ yielding the identity mapping but all distinct from the case of the uniform magnetic field. In particular, when $c \rightarrow 0$, we should have $A_c(0) \rightarrow 0$ by continuity. But here again the result proved in Appendix C yields a contradiction because an equilibrium that corresponds to the identity mapping and is infinitesimally close to the equilibrium $A=0$ cannot be smooth. Hence $\Delta \phi$ cannot be smooth if the VB equation has a nonunique solution at B . Furthermore, any second equilibrium produced by such a nonunique solution cannot be smooth, which contradicts step (3) where S is assumed to be smooth.

In summary, consideration of both possibilities (a) and (b) shows that the assumption of a smooth second equilibrium S cannot be sustained. Therefore we conclude that there exists at most only one smooth solution for a footpoint mapping connected continuously with the identity mapping. This completes the proof of the theorem stated in Sec. III.

Before we conclude this Appendix, we make a few additional remarks on the physical implications of our results. Now that we have shown that S cannot be a smooth equilibrium, it must be a nonequilibrium state with current sheet(s). Since it is a singular state, we cannot apply the VB equation to determine the consequences of the reverse footpoint drive $D(t)$. However, the branch BSS_∞ still exists and represents a sequence of nonsmooth states, obtained by relaxation from the unstable branch BFF_∞ .

The solution of the VB equation is nonunique at the marginal stability point B which is a bifurcation point⁴⁸ for a branch of unstable equilibrium (represented schematically by the curve BFF_∞) and a branch of stable equilibrium (curve BSS_∞). While we agree with Ref. 48 regarding the occur-

rence of such pitchfork bifurcations, the issue is whether as a result of such a bifurcation one obtains a branch BSS_∞ of smooth (and stable) equilibrium solutions. We propose that if the dynamics is constrained by the ideal MHD equations and topological change is forbidden, then BSS_∞ must be a minimum-energy branch of singular, nonequilibrium solutions containing current sheets.

An analogy with Taylor's model of turbulent relaxation⁴⁹ gives us further insight into the Parker problem. Taylor has shown that the force-free, axisymmetric equilibrium solution in a periodic cylinder, when unstable, can relax to a nonaxisymmetric solution. Note that although both solutions are smooth in Taylor's model, they are not connected by ideal MHD dynamics. Taylor invokes a small but finite resistivity η to permit change in the topology of field lines. He points out that as $\eta \rightarrow 0$, the field gradients must become very large. Therefore if the dynamics is constrained by ideal MHD ($\eta=0$), we expect that the magnetic field will tend to a singular state. Indeed, an ideal MHD plasma has an infinite number of topological invariants^{30,50} which enable, in principle, the construction of such singular solutions. The intervention of even a small amount of resistivity relaxes the topological constraints imposed by ideal MHD, and enables the relaxation process to find a smooth nonaxisymmetric state.

APPENDIX C: EQUILIBRIUM WITH IDENTITY MAPPING

For the theorem stated in Sec. III and proved in Appendix B, we have considered footpoint mappings that are connected smoothly to the identity mapping. The properties of a magnetostatic equilibrium with the identity mapping, invoked in Appendix B, are the subject of this Appendix.

Assume that there exist a smooth equilibrium with $A \neq 0$ satisfying Eq. (3) with periodic boundary conditions and the identity mapping from $z=0$ onto L . We first show:

An equilibrium obeying the identity mapping cannot be independent of z , unless it is a uniform magnetic field.

We choose $L=1$ without loss of generality. Then we can represent the equilibrium by the Fourier series

$$A = \sum_{lmn} A_{lmn} e^{2\pi i(lx + my + nz)},$$
(C1)

$$J = \sum_{lmn} J_{lmn} e^{2\pi i(lx + my + nz)},$$

with constant Fourier coefficients and $J_{lmn} = (2\pi)^2 (l^2 + m^2) A_{lmn}$. In particular, we can choose $A_{00n} = 0$ (for all n) since they only contribute an unimportant function of z .

Consider an equilibrium satisfying Eq. (3) with $\partial J / \partial z = [A, J] = 0$. (Here A is a function of x and y only.) Then A is analogous to the stream function of a steady, 2-D Euler flow. Following a field line from $z=0$ to L is equivalent to following the movement of a Lagrangian element of the analogous flow. For each field line we can identify such a fluid element. Each element must travel along a contour of constant A . In order to preserve the identity mapping, all the fluid elements which start their motion at the same time must

return to their starting points simultaneously. For the identity mapping, we cannot have a contour of A which is an open curve because that would require the direction in which every fluid element moves on the contour to change sign, which is impossible unless every fluid element is at rest at a fixed point, that is, $A=0$. Therefore all contours of A must be closed loops, and all the fluid elements must go around a loop at least once to return to their starting points. Now, two loops with the same direction of rotation cannot be neighbors because the flow direction is discontinuous along the shared border. Therefore the loops which correspond to different directions of rotation must form arrays of X points. However, since the mapping for an X point is not an identity mapping, we are led to a contradiction. Hence an equilibrium which is independent of z cannot obey the identity mapping unless $A=0$ and the magnetic field is uniform.

By the demonstration above, we cannot have $A_{lmn}=0$ for all $n \neq 0$. Now consider A to be infinitesimally close but not identically equal to zero. We must have $|A_{lmn}| \ll 1$ for all l, m, n . We also have

$$\int A^2 d^3x = \sum_{lmn} |A_{lmn}|^2 \equiv c^2 \ll 1, \quad (C2)$$

where the volume integral is over a unit cube. We will now show:

If A is infinitesimally close but not identically equal to zero, it cannot remain smooth as $c \rightarrow 0$.

We first give a plausible asymptotic argument. With $A \sim O(c)$, we obtain $\partial/\partial z \sim O(1)$ by Eq. (C1). Assume that $|\partial/\partial \mathbf{x}_\perp| \sim 1/\delta$. Substituting these orderings in Eq. (3), we obtain

$$\delta^2 \sim c \rightarrow 0, \quad (C3)$$

which means that the perpendicular length scale has to tend to zero. Hence, A cannot be a smooth equilibrium.

The qualitative asymptotic argument given above can be made more precise. Define $a_{lmn} = A_{lmn}/c$. We then have

$$\int \left(\frac{\partial J}{\partial z} \right)^2 d^3x = c^2 (2\pi)^6 \sum_{lmn} n^2 (l^2 + m^2)^2 |a_{lmn}|^2, \quad (C4)$$

and

$$\int [A, J]^2 d^3x = c^4 (2\pi)^8 \sum_{lmn} \left| \sum_{pqr} (p^2 + q^2) \times (lq - mp) a_{pqr} a_{l-p, m-q, n-r} \right|^2. \quad (C5)$$

By Eq. (3), the two quantities on the left-hand sides of Eqs. (C4) and (C5) must be equal. Since A is smooth by assumption, we should be able to represent the right-hand side of Eq. (C5) with a finite number of terms N . We obtain

$$(2\pi)^2 c^2 > \frac{\sum_{lmn} n^2 (l^2 + m^2)^2 |a_{lmn}|^2}{N \sum_{lmn}^N \sum_{pqr}^N (p^2 + q^2)^2 (lq - mp)^2} \equiv f(N) \neq 0. \quad (C6)$$

Equation (C6) implies that if $c \rightarrow 0$, we must have $N \rightarrow \infty$. In

other words, in the limit $c \rightarrow 0$, we need to sum over an infinite number of Fourier terms. Hence A cannot be smooth.

- ¹E. N. Parker, *Astrophys. J.* **174**, 499 (1972).
- ²A. A. van Ballegooijen, *Astrophys. J.* **298**, 421 (1985).
- ³S. K. Antiochos, *Astrophys. J.* **312**, 886 (1987).
- ⁴E. G. Zweibel and H.-S. Li, *Astrophys. J.* **312**, 423 (1987).
- ⁵D. W. Longcope and H. R. Strauss, *Astrophys. J.* **437**, 851 (1994).
- ⁶B. C. Low, *Annu. Rev. Astron. Astrophys.* **28**, 491 (1990).
- ⁷P. K. Browning, *Plasma Phys. Controlled Fusion* **33**, 539 (1991).
- ⁸E. N. Parker, *Spontaneous Current Sheets in Magnetic Fields* (Oxford University Press, New York, 1994).
- ⁹G. B. Field, in *Topological Fluid Mechanics*, edited by H. K. Moffatt and A. Tsinober (Cambridge University Press, Cambridge, England, 1990), p. 244.
- ¹⁰N. Otani and H. Strauss, *Astrophys. J.* **325**, 468 (1988).
- ¹¹H. R. Strauss and N. F. Otani, *Astrophys. J.* **326**, 418 (1988).
- ¹²Z. Mikic, D. D. Schnack, and G. Van Hoven, *Astrophys. J.* **338**, 1148 (1989).
- ¹³I. J. D. Craig and A. D. Sneyd, *Astrophys. J.* **357**, 653 (1990).
- ¹⁴D. W. Longcope and H. R. Strauss, *Astrophys. J.* **426**, 742 (1994).
- ¹⁵G. Van Hoven, Y. Mok, and Z. Mikic, *Astrophys. J.* **440**, L105 (1995).
- ¹⁶K. Galsgaard and A. Nordlund, *J. Geophys. Res.* **101**, 13445 (1996).
- ¹⁷A. W. Longbottom, G. J. Rickard, I. J. D. Craig, and A. D. Sneyd, *Astrophys. J.* **500**, 471 (1998).
- ¹⁸Z. W. Ma, C. S. Ng, X. Wang, and A. Bhattacharjee, *Phys. Plasmas* **2**, 3184 (1995).
- ¹⁹J. M. Finn and P. K. Kaw, *Phys. Fluids* **20**, 72 (1977).
- ²⁰A. Bhattacharjee, T. Hayashi, C. C. Hegna, N. Nakajima, and T. Sato, *Phys. Plasmas* **2**, 883 (1995).
- ²¹J. M. Greene, *J. Geophys. Res.* **93**, 8583 (1988).
- ²²Y.-T. Lau and J. M. Finn, *Astrophys. J.* **350**, 672 (1990).
- ²³J. M. Greene, in *Chaos and Order*, edited by N. Joshi and R. L. Dewar (World Scientific, Singapore, 1991), p. 49.
- ²⁴H. R. Strauss, *Phys. Fluids* **19**, 134 (1976).
- ²⁵T. Kato, *Arch. Ration. Mech. Anal.* **25**, 188 (1967).
- ²⁶T. Gold and F. Hoyle, *Mon. Not. R. Astron. Soc.* **120**, 89 (1960).
- ²⁷M. A. Raadu, *Sol. Phys.* **22**, 425 (1972).
- ²⁸R. Giachetti, G. Van Hoven, and C. Chiuderi, *Sol. Phys.* **55**, 371 (1977).
- ²⁹Z. Mikic, D. D. Schnack, and G. Van Hoven, *Astrophys. J.* **361**, 690 (1990).
- ³⁰M. D. Kruskal and R. M. Kulsrud, *Phys. Fluids* **1**, 265 (1958).
- ³¹H. K. Moffatt, *J. Fluid Mech.* **159**, 359 (1985).
- ³²P. R. Garabedian, *Partial Differential Equations* (Wiley, New York, 1964), p. 284.
- ³³S. C. Cowley, D. W. Longcope, and R. N. Sudan, *Phys. Rep.* **283**, 227 (1997).
- ³⁴E. N. Parker, *Cosmical Magnetic Fields* (Clarendon Press, Oxford, 1979), p. 359.
- ³⁵F. L. Waelbroeck, *Phys. Fluids B* **1**, 2372 (1989).
- ³⁶A. Bhattacharjee and X. Wang, *Astrophys. J.* **372**, 321 (1991).
- ³⁷D. W. Longcope and H. R. Strauss, *Phys. Fluids B* **5**, 2858 (1993).
- ³⁸H. R. Strauss, *Astrophys. J.* **381**, 508 (1991).
- ³⁹H. R. Strauss, *Geophys. Res. Lett.* **20**, 325 (1993).
- ⁴⁰D. W. Longcope and R. N. Sudan, *Astrophys. J.* **437**, 491 (1994).
- ⁴¹X. Wang and A. Bhattacharjee, *Astrophys. J.* **420**, 415 (1994).
- ⁴²M. A. Berger, in *Proceedings of an International Workshop on Space Plasmas, Potsdam, Germany* (European Space Agency, Paris, 1988), SP-285, Vol. II, 83.
- ⁴³H. Politano, A. Pouquet, and P. L. Sulem, *Phys. Plasmas* **2**, 2931 (1995).
- ⁴⁴E. R. Priest and P. Démoulin, *J. Geophys. Res.* **100**, 23443 (1995).
- ⁴⁵G. Van Hoven, D. L. Hendrix, and D. D. Schnack, *J. Geophys. Res.* **100**, 19819 (1995).
- ⁴⁶G. Hornig and L. Rastätter, *Phys. Scr.* **T74**, 34 (1998).
- ⁴⁷P. Hartman, *Ordinary Differential Equations* (Wiley, New York, 1964), pp. 418–435.
- ⁴⁸D. W. Longcope and R. N. Sudan, *Astrophys. J.* **384**, 305 (1992).
- ⁴⁹J. B. Taylor, *Rev. Mod. Phys.* **58**, 741 (1986).
- ⁵⁰A. Bhattacharjee, R. L. Dewar, and D. A. Monticello, *Phys. Rev. Lett.* **45**, 347 (1980).